IEEE Access
Multidisciplinary | Rapid Review | Open Access Journal

Received July 26, 2019, accepted August 22, 2019, date of publication September 3, 2019, date of current version September 17, 2019.

Digital Object Identifier 10.1109/ACCESS.2019.2939140

Approach Angle-Based Saturation Function of Modified Complementary Sliding Mode Control for PMLSM

HONGYAN JIN AND XIMEI ZHAO
School of Electrical Engineering, Shenyang University of Technology, Shenyang 110870, China
Corresponding author: Ximei Zhao (zhaoxm_sut@163.com)

This work was supported in part by the National Natural Science Foundation under Grant 51175349, and in part by the Key Projects of Liaoning Provincial Natural Science Foundation Plans under Grant 20170540677.

ABSTRACT In this paper, an approach angle-based saturation function of modified complementary sliding mode control (MCMSC) method was proposed to overcome the influence of uncertainties such as parameter variations and external disturbances on permanent magnet linear synchronous motor (PMLSM) servo system. On the foundation of the mathematical model considering uncertainties of PMLSM and the theory of sliding mode control (SMC), complementary sliding mode control (CSMC) method was designed by combining the integral sliding surface with the complementary sliding surface. By using the continuous saturation function, CSMC can efficiently eliminate the system chattering phenomenon caused by the discontinuous function in SMC and further improve the position tracking accuracy. However, the saturation function makes the boundary layer in CSMC constant, so the asymptotic stability of the system cannot be guaranteed. Hence, an approach angle-based saturation function of MCSMC was designed to realize the dynamic change of the boundary layer, which can diminish the boundary layer with the change of state trajectory until it converges to the sliding surface, thereby further improving the robustness of the system. Additionally, the hybrid SMC methods, such as fuzzy-SMC and neural network-SMC (NN-SMC), are avoided. A precise test platform based on digital signal processor (DSP) was implemented, and experimental results are shown to demonstrate the effectiveness and correctness of the proposed method.

INDEX TERMS Permanent magnet linear synchronous motor (PMLSM), uncertainties, complementary sliding mode control (CSMC), saturation function, approach angle.

I. INTRODUCTION

Permanent magnet linear synchronous motor (PMLSM) is an industry standard in fields such as microscale robotic, electronic assembly, machine tools and manufacturing [1], [2]. Compared with the rotary motor, PMLSM is very stiff and has a simpler mechanical construction, which can directly generate large electromagnetic thrust and reduce mechanical losses [3]. Therefore, high positioning accuracy and high speed performance of PMLSM can be achieved.

With the improvement of performance indexes in application fields, the precision requirement of PMLSM is continuous increasingly [4]. However, due to the elimination of mechanical transmission components, PMLSM is susceptible to time-varying uncertainties such as parameter variations and external disturbances [5], [6]. Consequently, the controller of the PMLSM servo system should be robust enough to tolerate these uncertainties. In order to suppress the uncertainties and achieve high-quality servo performance, researchers have focused on this area and have employed extensive studies for motor control such as the backstepping control in [7]–[9], neural network control in [10]–[12], and fuzzy control in [13], [14].

Compared with the control strategy above, sliding mode control (SMC) is now well recognized as a methodology capable of achieving strong robustness to uncertainties and fast dynamic response [15]. However, the good performance of SMC is usually guaranteed by using the large switching gain in the discontinuous control law. It will lead to chattering phenomenon which is caused by the discontinuous

The associate editor coordinating the review of this article and approving it for publication was Ton Do.

function in the control law, and the chattering may excite the neglected or un-modeled high-frequency dynamics [9], [16]. Thus, the way to reduce chattering has achieved much popularity.

To the authors' knowledge, rich literatures have been studied on the chattering problem in SMC. A common method adopted to eliminate chattering is to decrease the value of switching gain [17]. However, the constraint relationship between the switching gain and the robustness may enable the system to achieve poor robustness when the value of switching gain is small. To address this problem, some hybrid control strategies such as fuzzy-SMC and neural network-SMC (NN-SMC) are proposed to solve the chattering problem. In [18], a self-organizing fuzzy-SMC method is proposed for the position control of the permanent magnet synchronous motor (PMSM) drive. The proposed scheme does not require robust terms to compensate the uncertainties of system mathematical model. Hence, it can eliminate the chattering phenomenon of traditional SMC. In [19], [20], wavelet NN-SMC was proposed by Hsu and Sousy. By combining the learning capability of the artificial neural network with the strong robustness of SMC, the method can realize chattering-free control and achieve strong robustness. However, despite the good performance of the hybrid control strategy described above, the combination of controllers increases the complexity of the design and affects the dynamic response capability of the system.

An alternative solution to avoid using the discontinuous function is to replace the sign function with the saturation function [21]. By introducing the complementary generalized error transformation, Su and Wang proposed a complementary sliding mode control (CSMC) to replace the switching function of SMC to improve the tracking precision and reduce the chattering in [22]. In [23], CSMC is applied to control the mover position of PMLSM for the tracking of different trajectories. Though good tracking performance and strong robustness are achieved, the indefinite steady-state tracking error is caused mainly depending on the boundary layer thickness and the switching gain. Thus, the performance of the control system is acceptable when the parameter mismatch is small. However, large mismatch of parameters can lead to the increase of the steady-state error, the overshoot and the oscillation. In [24], [25], radial-basis-function neural network (RBFNN) and recurrent wavelet-based Elman neural network (RWENN) are combined with CSMC to solve the problem of parameter selection and further improve the robustness. Although the incorporation of saturation function is one of the effective methods to suppress chattering phenomenon, the state trajectory of the system cannot converge asymptotically to the sliding surface due to the constant thickness of the boundary layer. As a result, the system has poor robustness on the sliding surface.

In this study, a modified complementary sliding mode control (MCSMC) method, which incorporates an approach angle-based saturation function, is proposed to reduce chattering phenomenon and suppress the uncertainties on

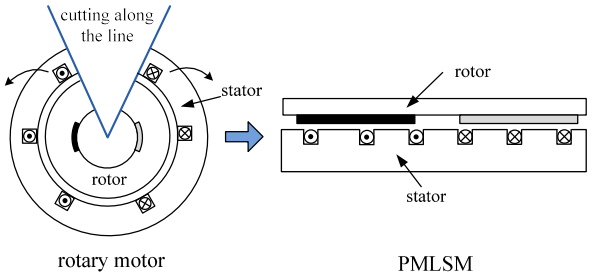

FIGURE 1. The structure of a rotary motor and a PMLSM.

PMLSM servo system. The approach angle in saturation function is as a measure of the orientation of the state trajectory with respect to the sliding surface, so that the boundary layer decreases gradually with the convergence of the state trajectory. Consequently, the dynamic change of boundary layer thickness is realized and the asymptotic stability of the system is achieved. By implementing on a 32-bit floating-point digital signal processor (DSP), TMS320 F2812, the effectiveness of the approach angle-based saturation function of MCSMC method for PMLSM servo system is verified by experimentation. From the experimental results, the proposed method possesses the advantages of good tracking accuracy and robustness for the tracking of different reference trajectories compared with CSMC and the hybrid controller (CSMC based on RWENN).

The following parts of this paper are organized as follows. The description and modeling of PMLSM are introduced in Section II. The design of CSMC and MCSMC are developed in Section III with a stability analysis. Section IV describes the experimental setup, a series of experimental studies and performance measurements. Some concluding remarks are summarized in Section V.

II. DESCRIPTION AND MODELING OF PMLSM

PMLSM is considered as a structure's evolution of PMSM. It can be seen as a rotary motor which is cut along the radial direction and expanded the circumference into a straight line [26]. The structure of a rotary motor and a PMLSM is shown in Fig.1. The structure diagram of PMLSM is depicted in Fig.2, which comprises a long stationary stator housing a sequence of permanent magnets with linear guidance rail and linear scale as well as a short moving primary mover containing the core-armature winding and Hall sensors. The interaction between magnetic field of secondary magnet and phase currents circulates in the mover accordingly produces electromagnetic thrust force [27]. In addition, the electromagnetic thrust force is applied directly to the mechanical system without intermediate coupling mechanism.

In the analysis of PMLSM vector control, the d-q axis model can be used without considering the saturation of magnetic circuit and the end effect. In the synchronous reference frame, the voltage equation and the flux equation are

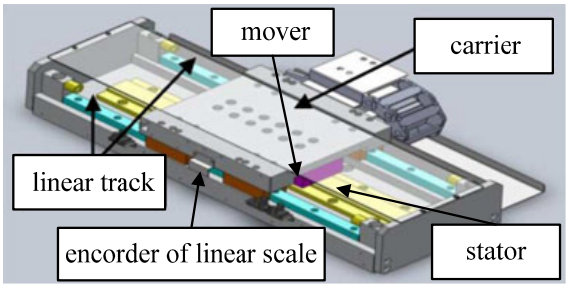

FIGURE 2. Structure diagram of PMLSM.

expressed as [28]

$$u_d = R_s i_d + \dot{\psi}_d - \omega\psi_q \tag{1}$$
$$u_q = R_s i_q + \dot{\psi}_q + \omega\psi_d \tag{2}$$
$$\psi_d = L_d i_d + \psi_f \tag{3}$$
$$\psi_q = L_q i_q \tag{4}$$

where u_d, u_q, i_d, i_q,L_d, L_q, ψ_d, ψ_q represent the voltage, current, inductance and flux of d-axis and q-axis, respectively, R_s is the resistance, ω is the angular velocity, and ψ_f is the flux of permanent magnets.

The electromagnetic thrust is expressed as

$$F_e = \frac{3\pi}{2\tau} p_n \left[\psi_f i_q + \left(L_d - L_q\right) i_d i_q\right] \tag{5}$$

where F_e is the electromagnetic thrust, τ is the pole pitch, p_n is the number of pole pairs.

In the surface mounted PMLSM,$L_d = L_q$, the electromagnetic thrust F_e can be simplified as

$$F_e = K_f i_q \tag{6}$$
$$K_f = 3\pi p_n \psi_f / 2\tau \tag{7}$$

where K_f is the thrust coefficient.

The mover dynamic equation of the PMLSM using the electromagnetic thrust shown in (6) can be

$$M\dot{v} = F_e - Bv - F_L \tag{8}$$

where M is the mass of the mover, B is the viscous friction coefficient, v is the linear velocity of the mover, F_L is lumped uncertainty including external disturbances, friction forces and parameter variations.

The following equation can be obtained by substituting (6) into (8)

$$\dot{v} = -Bv/M + K_f i_q/M - F_L/M \tag{9}$$

Assuming that the system parameter variations, friction forces and external disturbances are absent, i.e. $F_L = 0$, (9) can be rewritten as

$$\ddot{d} = -\frac{B}{M}\dot{d} + \frac{K_f}{M} i_q = a_n \dot{d} + b_n u \tag{10}$$

where d is the position of the mover, whose first derivative and second derivative represent the linear velocity v and acceleration of the mover, respectively, $a_n = -B/M$, $b_n = K_f/M > 0$, and $u = i_q$ is the control effort of the system.

Considering the existence of F_L, i.e. $F_L \neq 0$ in (9), (10) can be rewritten as

$$\begin{aligned}\ddot{d} &= (a_n + \Delta a)\,\dot{d} + (b_n + \Delta b)\,u + (c_n + \Delta c)\,F_L \\ &= a_n \dot{d} + b_n u + \beta\end{aligned} \tag{11}$$
$$\beta = \Delta a \dot{d} + \Delta b u + (c_n + \Delta c)\,F_L \tag{12}$$

where $c_n = -1/M$, Δa,Δb, Δc respectively denote the uncertainties introduced by the system parameters M and B, β is the lumped uncertainty and β is assumed to be bounded $|\beta| \leq \rho$, where ρ is a given positive constant and it is also considered as the switching gain of CSMC.

III. PROPOSED CONTROL SYSTEM

Since the PMLSM servo system is usually susceptible to the time-varying uncertainties, the controllers must be robust enough to the parameter variations, friction forces and external disturbances. It is well known that the major advantage of SMC is its insensible capability to uncertainties. Therefore, SMC is chosen as the basis of the controller design.

In this section, CSMC with traditional saturation function is designed first to reduce chattering and further improve the robustness. Subsequently, the approach angle is incorporated into the traditional saturation function to overcome the shortcomings of a sign function in SMC (excessive chattering) and a traditional saturation function in CSMC (does not ensure asymptotic stability). Finally, the approach angle-based MCSMC is proposed to realize the dynamic change of boundary layer and guarantee the asymptotic stability of the PMLSM servo system. An experimental system is established using a PMLSM, a DSP control board, an inverter, a rectifier, and other elements to verify the effectiveness of the proposed MCSMC. The block diagram of PMLSM servo system using MCSMC based on DSP is shown in Fig.3.

A. CSMC DESIGN

For the PMLSM servo system, it is desired to design the controller to track different reference trajectories. To simplify the design, the position tracking error is defined as

$$e = d_m - d \tag{13}$$

where d_m is the reference input signal, d is the position of the mover, e is the position tracking error.

CSMC is the combination of complementary sliding surface with the integral sliding surface, so as to achieve performance optimization. The existence condition of sliding surface is that the system state can reach the sliding surface in finite time. The arrival condition of sliding mode is defined as

$$\lim_{s\to 0^+} \dot{s} < 0,\ \lim_{s\to 0^-} \dot{s} > 0 \, or \, s\dot{s} < 0 \tag{14}$$

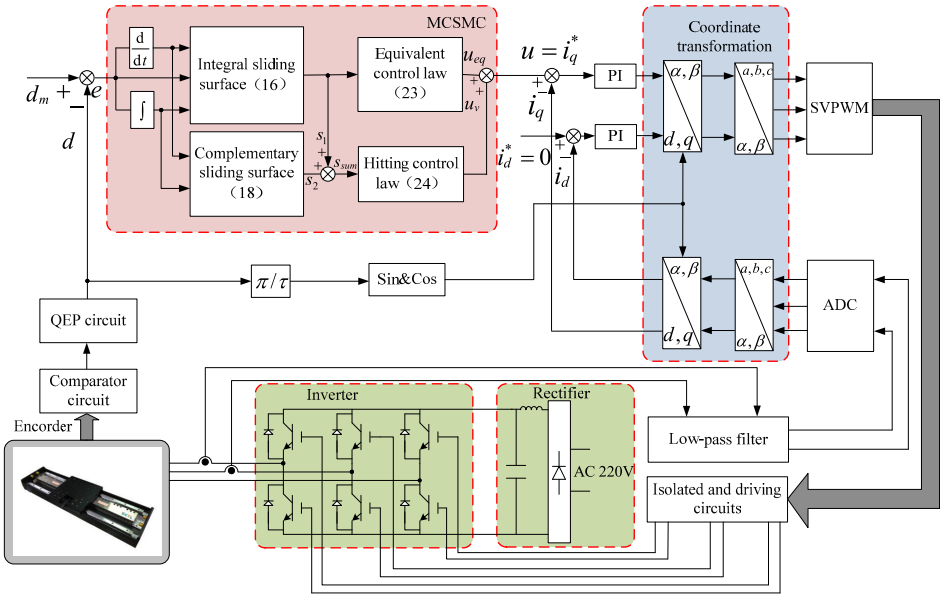

FIGURE 3. Block diagram of PMLSM servo system using MCSMC based on DSP.

In order to ensure the arrival within finite time and avoid asymptotic approximation, (14) can be modified as [29]

$$\begin{cases} \dot{s} > \varepsilon, \ s < 0 \\ \dot{s} < \varepsilon, \ s > 0 \end{cases} \quad or \ s\dot{s} < -\varepsilon \left| s \right| \tag{15}$$

where $\varepsilon > 0$, which is a neighborhood of the sliding surface. The smaller of ε, the closed the state is constrained to the actual sliding surface, which enables the system state point to reach the sliding surface in finite time.

The dynamic behavior of the system may be tailored by the particular choice of the switching surface. According to the arrival condition, the integral sliding surface of CSMC is defined as

$$s_1 = \dot{e} + 2\lambda e + \lambda^2 \int_0^t e d\tau \tag{16}$$

where s_1 is the integral sliding surface of CSMC, λ is a given positive constant. The following equation can be obtained by substituting (11) and (13) into (16) and taking the derivative

$$\begin{aligned} \dot{s}_1 &= \ddot{e} + 2\lambda\dot{e} + \lambda^2 e \\ &= \left(\ddot{d}_m - a_n\dot{d} - b_n u - \beta\right) + 2\lambda\dot{e} + \lambda^2 e \end{aligned} \tag{17}$$

Integral sliding surface is an integral term of state variables added on the basis of linear sliding surface. The introduction of integral term can eliminate the steady-state error of the system and improve the tracking performance of the system [30]. However, it will also delay the response time of the system. Hence, the complementary sliding surface is designed to compensate the deficiencies. The complementary sliding surface is designed as

$$s_2 = \dot{e} - \lambda^2 \int_0^t e d\tau \tag{18}$$

where s_2 is the complementary sliding surface.

On account of the same constant λ existing in the two sliding surfaces, the relationship between s_1 and s_2 can be obtained as follows

$$\dot{s}_2 + \lambda(s_1 + s_2) = \dot{s}_1 \tag{19}$$

The goal in CSMC is to design a control law to drive the system states to the sliding surface in a finite time, and then to maintain the condition for all the future time. To address the task, the control law u of CSMC involves equivalent control law u_{eq} and hitting control law u_v, which is mainly to realize robust control of uncertainties.

In order to ensure the stability of the system, the first Lyapunov function candidate for the CSMC system is chosen as

$$V = \frac{1}{2}\left(s_1^2 + s_2^2\right) \tag{20}$$

The following equation can be obtained by taking the time derivative of (20) and using (17)-(19)

$$\begin{aligned} \dot{V} &= s_1\dot{s}_1 + s_2\dot{s}_2 \\ &= (s_1 + s_2)\left[\ddot{d}_m - a_n\dot{d} - b_n u - \beta + 2\lambda\dot{e} + \lambda^2 e - \lambda s_2\right] \end{aligned} \tag{21}$$

According to (21), a CSMC control law u is designed as follows

$$u = u_{eq} + u_v \tag{22}$$

$$u_{eq} = \frac{1}{b_n}\left[\ddot{d}_m - a_n\dot{d} + \lambda(2\dot{e} + \lambda e + s_1)\right] \tag{23}$$

$$u_v = \frac{1}{b_n}\left[\rho \mathrm{sat}(\frac{s_1 + s_2}{\varphi})\right] \tag{24}$$

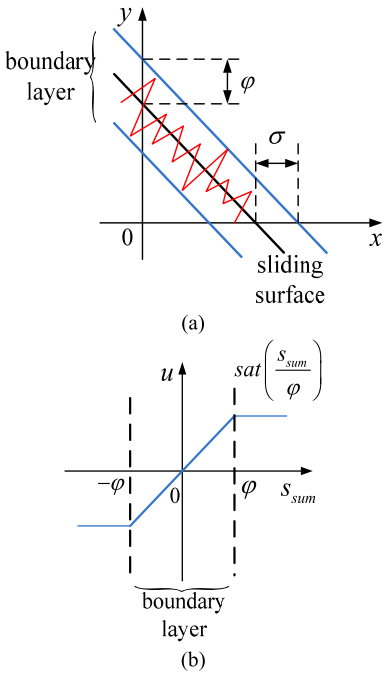

FIGURE 4. Diagram of boundary layer in CSMC.

where u_{eq} is the equivalent control law, which is desired to keep the system state on the sliding surface, u_v is the hitting control law. φ is the boundary layer thickness, and sat$(\cdot)$ is the saturation function. It is designed as follows

$$\text{sat}(\frac{s_1+s_2}{\varphi}) = \begin{cases} 1, & s_1+s_2 \geq \varphi \\ \dfrac{s_1+s_2}{\varphi}, & -\varphi < s_1+s_2 < \varphi \\ -1, & s_1+s_2 \leq -\varphi \end{cases} \quad (25)$$

B. MCSMC DESIGN

CSMC with traditional saturation function can effectively suppress the influence of lumped uncertainties and ensure the robustness of PMLSM servo system. However, due to the constant thickness of the boundary layer, the trajectory of the system can only converge within the boundary layer rather than the sliding surface. The diagram of the boundary layer in CSMC is shown in Fig.4.

Where σ is the width of the boundary layer. It can be seen from Fig.4 (b) that the boundary $s_{sum} = \varphi$ and $s_{sum} = -\varphi$ are on both sides of the sliding surface $s_{sum} = 0$. As for the adoption of the feedback linearization control on the boundary layer, the system state trajectory cannot converge to the switching surface within a finite time, which is likely to reduce the global robustness of the system. Therefore, an approach angle-based saturation function has to be designed to control the dynamic boundary layer of the system.

The following equation can be obtained by defining the sliding surfaces summation variable

$$s_{sum} = s_1 + s_2 \quad (26)$$

where s_{sum} is the sum of the sliding surfaces.

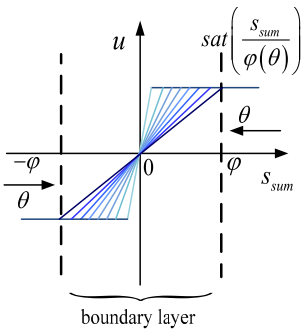

FIGURE 5. Diagram of dynamic boundary layer in MCSMC.

Equation (25) can be rewritten by using (26)

$$sat(\frac{s_{sum}}{\varphi}) = \begin{cases} 1, & s_{sum} \geq \varphi \\ \dfrac{s_{sum}}{\varphi}, & -\varphi < s_{sum} < \varphi \\ -1, & s_{sum} \leq -\varphi \end{cases} \quad (27)$$

Equation (27) can be rewritten by simplification

$$sat\left(\frac{s_{sum}}{\varphi}\right) = \begin{cases} \dfrac{s_{sum}}{\varphi}, & \left|\dfrac{s_{sum}}{\varphi}\right| \leq 1 \\ sat\left(\dfrac{s_{sum}}{\varphi}\right), & \left|\dfrac{s_{sum}}{\varphi}\right| > 1 \end{cases} \quad (28)$$

It can be seen from (28) that sat$(\cdot)$ is a traditional continuous switching function, which is used to replace the discontinuous function in SMC. By using the saturation function, the excessive chattering caused by the discontinuous control law can be eliminated.

In order to solve the problem that the thickness of boundary layer is fixed by traditional saturation function and the CSMC system cannot be asymptotically stable, the approach angle-based saturation function is defined as [31]

$$\text{sat}\left(\frac{s_{sum}}{\varphi(\theta)}\right) = \begin{cases} \dfrac{s_{sum}}{\varphi(\theta)}, & \left|\dfrac{s_{sum}}{\varphi(\theta)}\right| \leq 1 \\ \text{sat}\left(\dfrac{s_{sum}}{\varphi(\theta)}\right), & \left|\dfrac{s_{sum}}{\varphi(\theta)}\right| > 1 \end{cases} \quad (29)$$

where θ is the approach angle, which is a measure of the orientation of the state trajectory with respect to the sliding surface. The diagram of the dynamic boundary layer in MCSMC is shown in Fig.5.

As shown in Fig.5, the boundary layer thickness φ is a dynamic variable related to θ. The relationship between φ and θ is as follows

$$\varphi = \frac{1}{\tan(\pi/2-\theta)} = \tan(\theta) \quad (30)$$

When the state trajectory of the system reaches the boundary layer, θ decreases gradually and the gradient of $sat(s_{sum}/\varphi(\theta))$ increases, making the boundary layer approach the switching surface. Under the condition of $|\theta| \rightarrow 0$, $sat(s_{sum}/\varphi(\theta))$ will increase infinitely, and

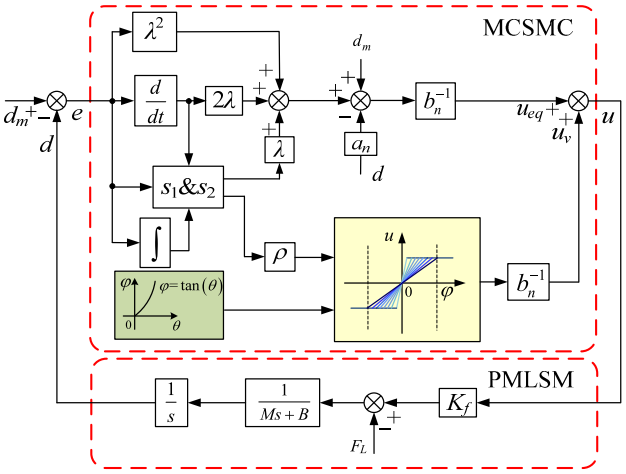

FIGURE 6. Structure diagram of PMLSM servo system using MCSMC.

the approach angle-based saturation function will reach an asymptotically stable state, i.e.

$$\lim_{|\theta|\to 0} sat\left(\frac{s_{sumi}}{\varphi(\theta)}\right) = \mathrm{sgn}(s_{sum}) \tag{31}$$

It can be seen from (31) that the approach angle-based saturation function approximates to the sign function. By incorporating the approach angle into the continuous switching term, the continuous switching term behaves similar to a discontinuous switching term, as the state trajectory nears the sliding surface. The structure diagram of PMLSM servo system using approach angle-based saturation function of MCSMC is shown in Fig.6.

To demonstrate the stability of the control scheme, the Lyapunov function is chosen as the same as the CSMC system, the following equation can be obtained by using (21-24), (26) and (29)

$$\begin{aligned}\dot{V} &= s_1\dot{s}_1 + s_2\dot{s}_2 \\ &= (s_1+s_2)\left[\ddot{d}_m - a_n\dot{d} - b_n u - \beta + 2\lambda\dot{e} + \lambda^2 e - \lambda s_2\right] \\ &= s_{sum}(-b_n u_v) - \lambda s_{sum}^2 + s_{sum}(-\beta) \\ &\le s_{sum}(-b_n u_v) - \lambda s_{sum}^2 + |s_{sum}|(|\beta|) \\ &\le -\lambda s_{sum}^2 + |s_{sum}|(|\beta| - \rho) \\ &= -\lambda s_{sum}^2 - \eta|s_{sum}| \\ &\le 0\end{aligned} \tag{32}$$

where η is a positive constant. Using the concept in [32], the system state will reach the sliding surface in a finite time smaller than $s_{sum}(t=0)/\eta$. This ensures that any system state trajectory starting outside the boundary layer, $|s_{sum}| \ge \varphi$, will reach the boundary layer in a finite time and slide along the intersection of the two sliding surfaces to the neighborhood of the zero point. Once the system state point reaches the sliding surface, the tracking error will approach zero in a finite time. Thus, incorporating the approach angle in MCSMC can achieve asymptotic stability while minimizing system chattering, without requiring a hybrid control structure such as fuzzy-SMC and NN-SMC. The convergence trajectory of MCSMC is shown in Fig.7.

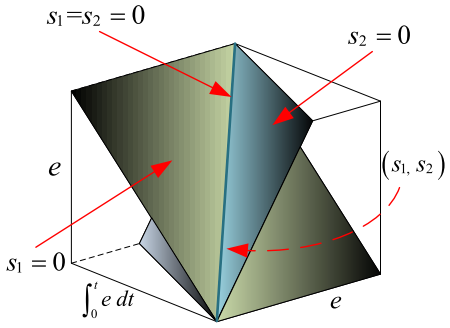

FIGURE 7. Convergence trajectory of CSMC.

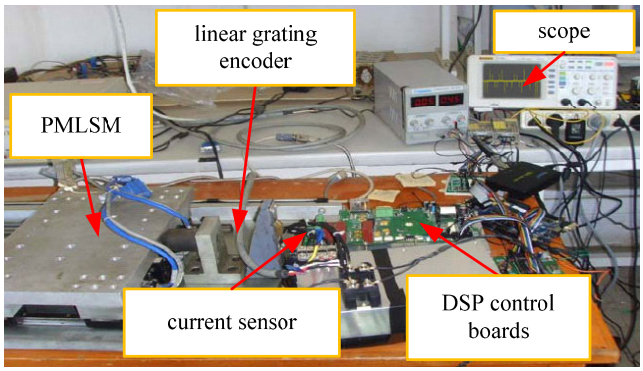

FIGURE 8. Experimental setup of control system.

TABLE 1. Parameters of CSMC and MCSMC.

Item and Symbol	Value (CSMC)	Value (MCSMC)
positive constant λ	130	150
switching control gain ρ	8	5
boundary thickness φ	0.05	—
approach angle θ	—	(0°,90°)

IV. EXPERIMENTAL RESULTS

A. EXPERIMENT SETUP AND PARAMETERS

To test the feasibility and the validity of the proposed method applied to the PMLSM servo system in practical applications, a PMLSM servo system based on DSP, TMS320 F2812 experiment platform is set up in Fig.8. The control object of the experimental system is the PMLSM produced by Kollmorgen, American, its maximum distance can be reached 260mm. The control chip is TMS320 F2812 DSP produced by Texas Instruments with fast computation and a completely integrated motor peripheral circuit, which is specially designed for motor control. The power conversion unit is PS21865 IPM (20A/600V) produced by Mitsubishi, Japan. It has a built-in IGBT drive circuit, overload protection

TABLE 2. Experimental cases of PMLSM servo system.

Condition / Controller	Case	Reference trajectory	Disturbance	Actual mover mass M_a	Actual vicious friction coefficient B_a
CSMC&MCSMC	Case1 (parameter variation)	sinusoidal	0 N	M_a=2M	B_a=1.5B
	Case2 (external disturbance)	trapezoidal	50 N	M_a=M	B_a=B
CSMC based on RWENN& MCSMC	Case3 (external disturbance)	step	50 N	M_a=M	B_a=B
	Case4 (load variation)	trapezoidal	variable	M_a=M	B_a=B

and power supply under-voltage protection function, all of those can contribute to the reliable operation of the system. Three-phase current signals of PMLSM are obtained by LT 58-S7 Hall current sensors to constitute a current feedback control with a ratio of 1000:1. In addition, the linear grating sensor with resolution 1 μm is used to detect position of the moving table. MicorE linear grating sensor is MII1600, which is used to detect position and velocity signals and feed them back to the system.

The main parameters of PMLSM servo system are given as: $R_s = 2.1\ \Omega$, $\psi_f = 0.09\ Wb$, $L_d = L_q = 41.4\ mH$, $\tau = 32\ mm$, $p_n = 3$, $K_f = 50.7\ N/A$, $M = 16.4\ kg$, $B = 8.0\ N{\cdot}s/m$. The parameters in CSMC and MCSMC are listed in Table 1. For the selection of parameters in CSMC, the trial-and-error method is adopted to obtain the control performance by continuously debugging parameters. All the parameters are selected to obtain the best dynamic and steady-state performance in experimentation considering the requirement of stability and possible operating conditions.

B. EXPERIMENTAL RESULTS AND ANALYSIS

In order to verify the effectiveness of the proposed method, CSMC with traditional saturation function in [23] and the hybrid controller (CSMC based on RWENN) in [25] are applied to the PMLSM servo system for the comparison of the control performance. In accordance with the conditions of reference trajectories, parameter variation, external disturbance and load variation, the cases of the comparative experiments are shown in table 2.

In case 1, to verify the dynamic tracking performance of MCSMC, a sinusoidal signal with a given amplitude of 10 mm and a period of π is carried out on the system at parameter variation condition. Since the actual position response curves coincide with the reference trajectory, only the position tracking error curves of the PMLSM servo system when using CSMC and MCSMC are shown in Fig.9(a) and Fig.9(b), respectively. In addition, the control effort curves of CSMC and MCSMC are shown in Fig.10(a) and Fig.10(b), respectively. The performance measures of case1 are illustrated in Table 3. The maximum tracking error, TE_{max}, the average tracking error, TE_{mean} can easily demonstrate the control performance, and the standard

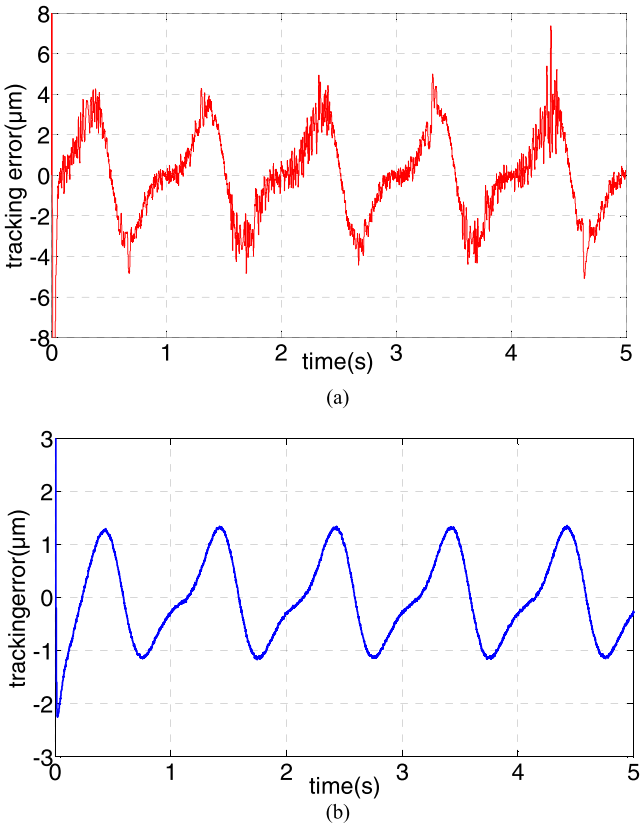

FIGURE 9. Position tracking error curves of PMLSM servo system at case 1 when using (a) CSMC (b) MCSMC.

deviation of the tracking error, TE_{sd}, can testify the oscillation of the tracking error. $TE_{max,}$, TE_{mean} and TE_{sd} are demonstrated as follows [33]

$$TE_{\max} = \max_k \sqrt{e(k)^2} \tag{33}$$

$$TE_{mean} = \sum_{k=1}^{n} \frac{e(k)}{n} \tag{34}$$

$$TE_{sd} = \sqrt{\sum_{k=1}^{n} \frac{(e(k) - TE_{mean})^2}{n}} \tag{35}$$

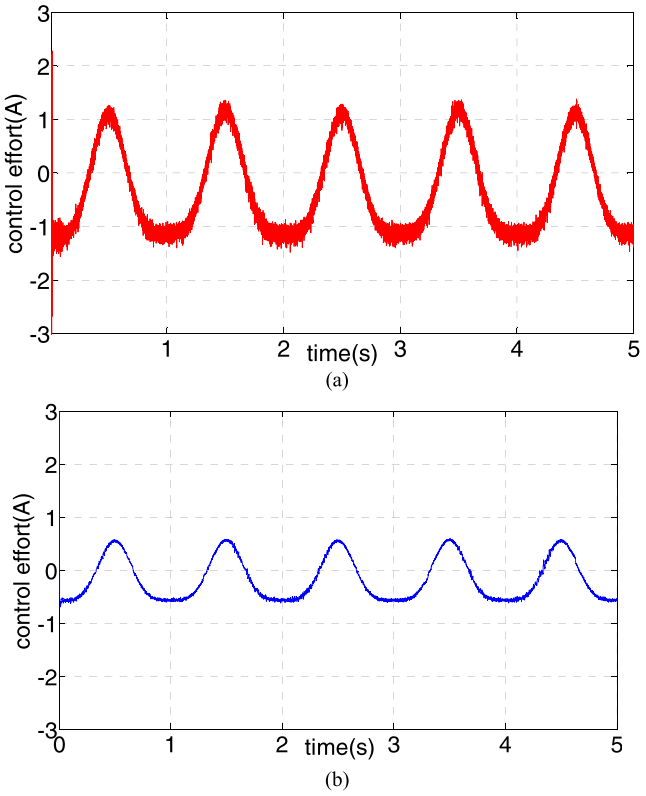

FIGURE 10. Control effort curves of PMLSM control system at case 1 when using (a) CSMC (b) MCSMC.

TABLE 3. Performance measures of case 1.

Value / Controller	Tracking errors(μm)		
	TE_{max}	TE_{mean}	TE_{sd}
CSMC	7.582	-0.089	0.487
MCSMC	1.375	-0.034	0.229

TABLE 4. Performance measures of case 2.

Value / Controller	Tracking errors(μm)		
	TE_{max}	TE_{mean}	TE_{sd}
CSMC	8.665	0.043	0.802
MCSMC	1.354	0.005	0.098

To further verify the robustness performance of MCSMC, the disturbance rejection is also investigated with an experiment in case 2. The position tracking curves and the tracking error curves of PMLSM servo system when using CSMC and MCSMC are shown in Fig.11 and Fig.12, respectively. Additionally, the control effort curves at case 2 are shown in Fig.13. The performance measures of case 2 are illustrated in Table 4.

Comparing the performance measures shown in Table 3 and Table 4, the TE_{max}, TE_{mean} and TE_{sd} of CSMC are reduced

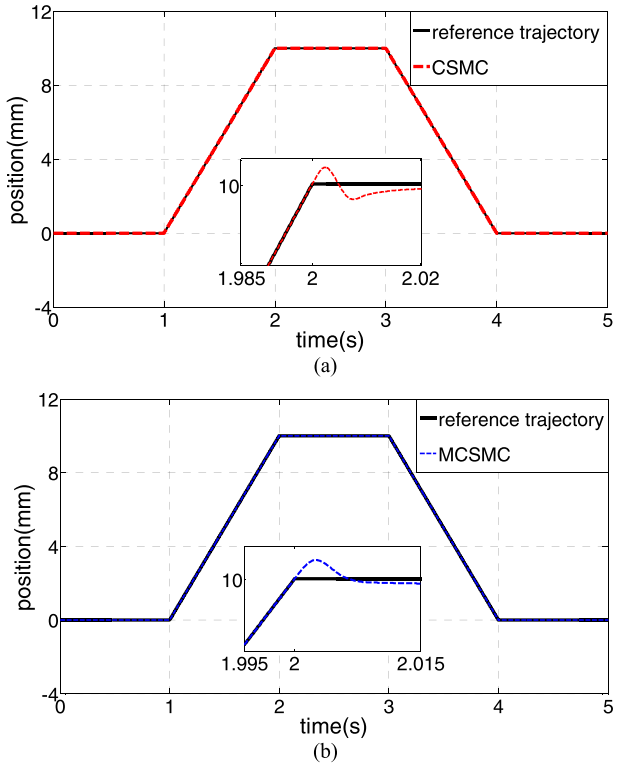

FIGURE 11. Position tracking curves of PMLSM servo system at case 2 when using (a) CSMC (b) MCSMC.

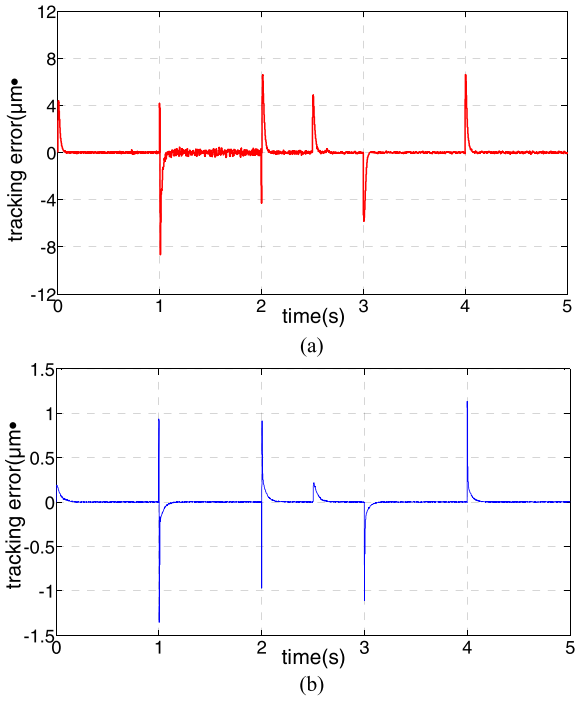

FIGURE 12. Position tracking error curves of PMLSM control system at case 2 when using (a) CSMC (b) MCSMC.

by 81.86%, 64.79% and 52.98%, at case 1, 84.37%, 88.37%, 87.78%, at case 2, respectively, with respect to MCSMC.

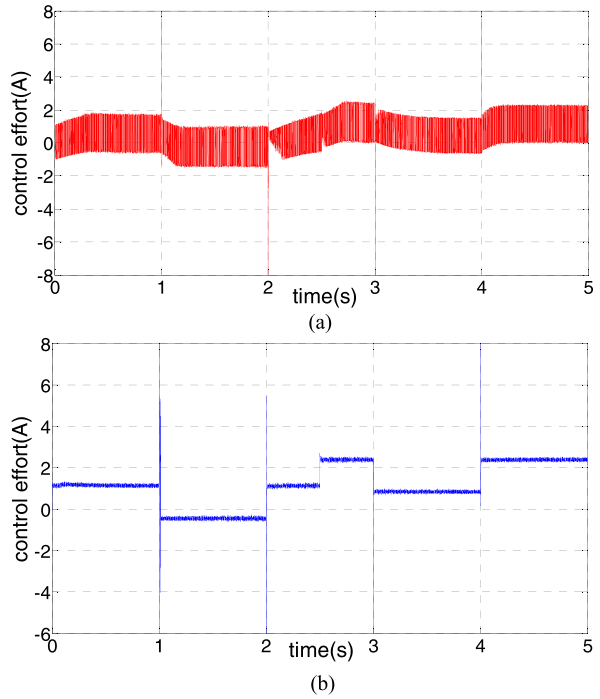

FIGURE 13. Control effort curves of PMLSM control system at case 2 when using (a) CSMC (b) MCSMC.

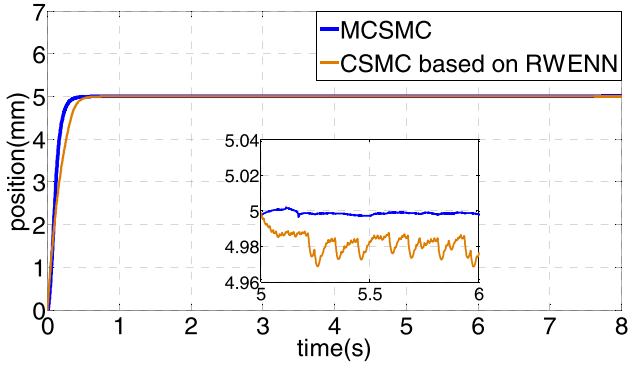

FIGURE 14. Position tracking curves of PMLSM servo system at case 3.

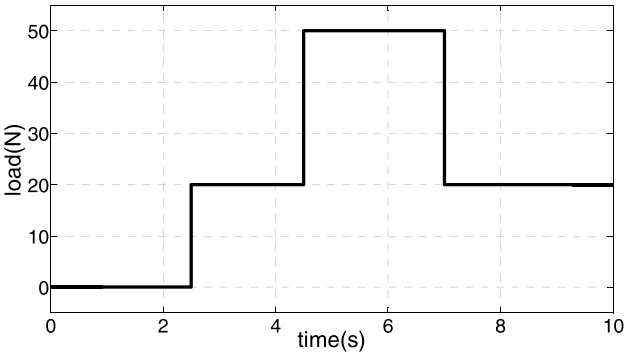

FIGURE 15. Load variation curve at case 4.

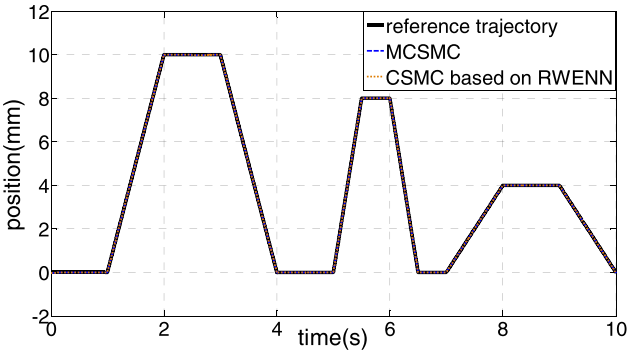

FIGURE 16. Position tracking curves of PMLSM servo system at case 4.

TABLE 5. Performance measures of case 4.

Value / controller	Tracking errors(μm)		
	TE_{max}	TE_{mean}	TE_{sd}
CSMC based on RWENN	7.504	0.224	1.141
MCSMC	6.989	0.163	0.610

Therefore, compared with CSMC, MCSMC can efficiently reduce the tracking error under the parameter variation condition and the external disturbance condition. In addition, by observing Fig.10 and Fig.13, it is obvious that the control effort curves of MCSMC is smoother. Despite the small chattering in the curve, it presents better control performance in contrast with CSMC. Therefore, MCSMC is potential to improve the tracking accuracy and eliminate the chattering phenomenon of the PMLSM servo system.

In case 3, a hybrid controller (CSMC based on RWENN) is applied for comparison. The RWENN is a dynamic neural network, which possesses strong on-line learning ability. It contains input layer (2 neurons), context layer (9 neurons), hidden layer (9 neurons) and output layer (1 neuron). By combining RWENN with the CSMC, the uncertainties of PMLSM servo system are estimated and the parameters are adjusted on-line. Thus, the robustness are achieved in [25]. Unlike the above method, the proposed MCSMC was designed by incorporating an approach angle into the traditional saturation function. It not only improves the performance of the system, but also avoids the hybrid control strategy such as fuzzy-SMC and NN-SMC. By giving the reference step signal under subsequent loading of 50 N, the dynamic performance of the PMLSM servo system is verified. The position response curves of CSMC based on RWENN and the proposed method are shown in Fig.14. By observing the system response at initial time, it is distinct that the proposed MCSMC provides a rapid and accurate response. In addition, there is no obvious overshoot under both control methods. To verify the robustness of the proposed method, 50 N is added to the system at 5 s. By comparing the zoomed maps of the position tracking curves at 5 s-6 s, it can be seen that the tracking curve of the motor under the CSMC based on RWENN shows obvious fluctuations when disturbed, while the one under MCSMC is comparatively smoother. As a result, the proposed MCSMC

TABLE 6. Comparison of different control schemes.

Characteristic / Controller	Tracking performance	Robustness	Response time	Chattering phenomenon	Learning ability
CSMC	middle	middle	favorable	middle	none
CSMC based on RWENN	favorable	favorable	poor	favorable	on-line
MCSMC	favorable	favorable	favorable	superior	none

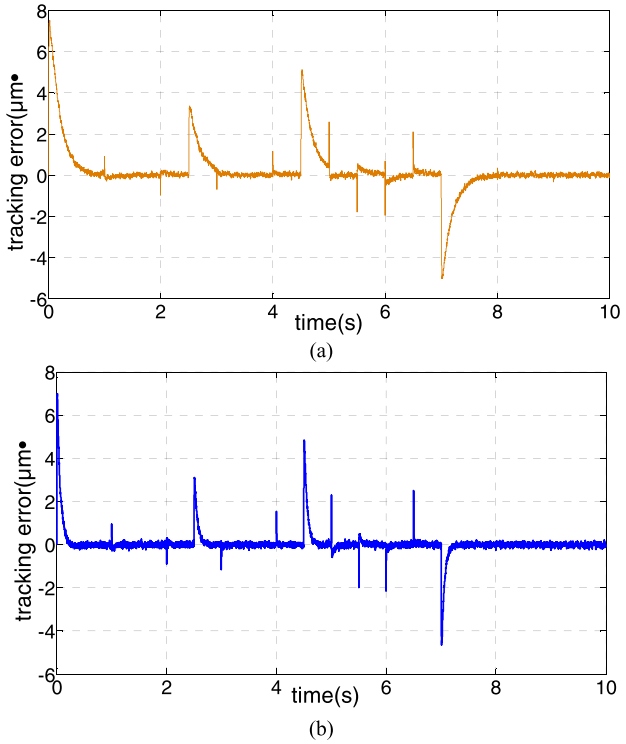

FIGURE 17. Position tracking error curves of PMLSM control system at case 4 when using (a) CSMC based on RWENN (b) MCSMC.

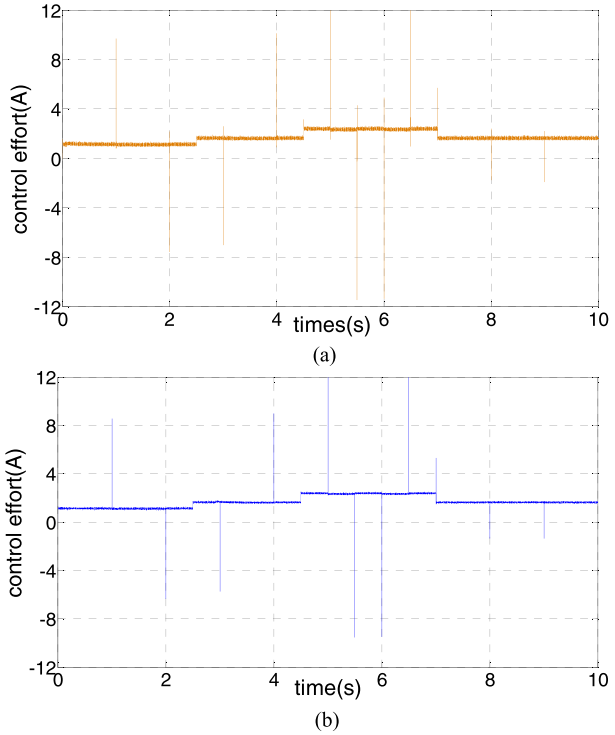

FIGURE 18. Control effort curves of PMLSM control system at case 4 when using (a)CSMC based on RWENN (b) MCSMC.

can yield superior performance than the CSMC based on RWENN.

To further evaluate the performance of MCSMC, the load variation condition is given to compare the performance between CSMC based on RWENN and MCSMC in case 4. The variable load curve is shown in Fig.15. The position response curves, the tracking error curves and control effort curves are shown in Fig.16, Fig.17 and Fig.18, respectively. It can be seen clearly that the better transient response and smaller oscillation are obtained by using MCSMC. For a clear presentation, the performance measures of case 4 are illustrated in Table 5. Comparing the performance measures shown in Table5, the TE_{max}, TE_{mean} and TE_{sd} of the CSMC based on RWENN are reduced by 6.86%, 27.23%, 46.54%, at case 4, respectively, with respect to MCSMC.

Through the analysis and comparison of the above experimental results, the comparison of different control schemes, CSMC, CSMC based on RWENN, MCSMC, are summarized in TABLE 6. Comparing the performance indexes in Table 6, it is obvious that the proposed MCSMC has superior control performance to control the mover position when uncertainties occur. Therefore, MCSMC can control a highly nonlinear PMLSM servo system effectively for practical applications.

V. CONCLUSION

This paper has proposed a reliable control strategy for PMLSM servo system which guarantees the robustness in the presence of the uncertainties. By incorporating the approach angle into the saturation function, the boundary layer can change gradually with the convergence of state trajectory, thus satisfying the asymptotic stability of the system. From the experimental results, the response of the system is fast enough and MCSMC has satisfactory performance in robustness for dealing with uncertainties. As a consequence,

the proposed MCSMC is of great significance in practical application. For further works, the following issues are deserved to be considered.

(1) In the designed controller, the friction force is considered as a part of the lumped uncertainty, and the influence of friction force on the system is not properly analyzed.

(2) The disadvantage of this control method is that it can only be applied to the case where the trajectory of the state moves towards the switching surface. That is to say, the range of the state trajectory approach angle is bounded as (0°, 90°).

REFERENCES

[1] F. Zhi, M. Zhang, Y. Zhu, and X. Li, "Analysis and elimination of harmonics in force of ironless permanent magnet linear synchronous motor," *Proc. CSEE*, vol. 37, no. 7, pp. 2101–2109, Apr. 2017.

[2] W.-T. Su and C.-M. Liaw, "Adaptive positioning control for a LPMSM drive based on adapted inverse model and robust disturbance observer," *IEEE Trans. Power Electron.*, vol. 21, no. 2, pp. 505–517, Mar. 2006.

[3] M.-Y. Chen and J.-S. Lu, "High-precision motion control for a linear permanent magnet iron core synchronous motor drive in position platform," *IEEE Trans Ind. Informat.*, vol. 10, no. 1, pp. 99–108, Feb. 2014.

[4] N. T.-T. Vu, D.-Y. Yu, H. H. Choi, and J.-W. Jung, "T–S fuzzy-model-based sliding-mode control for surface-mounted permanent-magnet synchronous motors considering uncertainties," *IEEE Trans. Ind. Electron.*, vol. 60, no. 10, pp. 4281–4291, Oct. 2013.

[5] E.-J. Park, S.-Y. Jung, and Y.-J. Kim, "A design of optimal interval between armatures in long distance transportation PMLSM for end cogging force reduction," *J. Elect. Eng. Technol.*, vol. 11, no. 2, pp. 361–366, Mar. 2016.

[6] X. Han, Q. Kun, and Z. Zhe, "Analysis and suppression measures of magnetic resistance force in permanent magnet linear synchronous motors," *Trans. China Electrotech. Soc.*, vol. 30, no. 6, pp. 70–76, Apr. 2015.

[7] J.-P. Yu, Y. Ma, B. Chen, and H.-S. Yu, "Adaptive fuzzy backstepping position tracking control for permanent magnet synchronous motor," *Control Decis.*, vol. 7, no. 4, pp. 1589–1601, Apr. 2010.

[8] F.-J. Lin, R.-J. Wai, W.-D. Chou, and S.-P. Hsu, "Adaptive backstepping control using recurrent neural network for linear induction motor drive," *IEEE Trans. Ind. Electron.*, vol. 49, no. 1, pp. 134–146, Feb. 2002.

[9] R. Trabelsi, A. Khedher, M. F. Mimouni, and F. M'sahli, "Backstepping control for an induction motor using an adaptive sliding rotor-flux observer," *Electr. Power Syst. Res.*, vol. 93, pp. 1–15, Dec. 2012.

[10] C. Li, G. Wang, Y. Li, and A. Xu, "Robust adaptive neural network control for switched reluctance motor drives," *Automatika*, vol. 59, no. 1, pp. 24–34, Jul. 2018.

[11] Z. Zhou, J. Yu, H. Yu, and C. Lin, "Neural network-based discrete-time command filtered adaptive position tracking control for induction motors via backstepping," *Neurocomputing*, vol. 260, pp. 203–210, Oct. 2017.

[12] C. Fu, L. Zhao, J. Yu, H. Yu, and C. Lin, "Neural network-based command filtered control for induction motors with input saturation," *IET Control Theory Appl.*, vol. 11, no. 15, pp. 2636–2642, Oct. 2017.

[13] G. G. Rigatos, "Adaptive fuzzy control for field-oriented induction motor drives," *Neural Comput. Appl.*, vol. 21, no. 1, pp. 9–23, Feb. 2012.

[14] E. A. Ramadan, M. El-Bardini, and M. A. Fkirin, "Design and FPGA-implementation of an improved adaptive fuzzy logic controller for DC motor speed control," *Ain Shams Eng. J.*, vol. 5, no. 3, pp. 803–816, Sep. 2014.

[15] J. Su, T. Li, and G. Yang, "Chattering phenomenon analysis and suppression of sliding mode observer in PMSM sensorless control," *Trans. China Electrotech. Soc.*, vol. 24, no. 8, pp. 58–64, Aug. 2009.

[16] J. Fei and X. Liang, "Adaptive backstepping fuzzy neural network fractional-order control of microgyroscope using a nonsingular terminal sliding mode controller," *Complexity*, vol. 2018, Sep. 2018, Art. no. 5246074.

[17] H. Lee and V. I. Utkin, "Chattering suppression methods in sliding mode control systems," *Annu. Rev. Control*, vol. 31, no. 2, pp. 179–188, 2007.

[18] Y. Guo and H. Long, "Self organizing fuzzy sliding mode controller for the position control of a permanent magnet synchronous motor drive," *Ain Shams Eng. J.*, vol. 2, no. 2, pp. 109–118, Jun. 2011.

[19] F. F. M. El-Sousy, "Robust wavelet-neural-network sliding-mode control system for permanent magnet synchronous motor drive," *IET Electr. Power Appl.*, vol. 5, no. 1, pp. 113–132, Jan. 2011.

[20] C.-F. Hsu and C.-H. Wang, "Chattering-free adaptive wavelet neural network control for a BLDC motor via dynamic sliding-mode approach," *Adv. Neural Netw. Res. Appl.*, vol. 67, pp. 773–781, 2010.

[21] X. Zhao and H. Jin, "Complementary sliding mode control for permanent magnet linear synchronous motor based on Elman neural network," *Trans. China Electrotech. Soc.*, vol. 33, no. 5, pp. 220–226, Mar. 2018.

[22] J.-P. Su and C.-C. Wang, "Complementary sliding control of non-linear systems," *Int. J. Control*, vol. 75, no. 5, pp. 360–368, Nov. 2002.

[23] X. Zhao and J. Zhao, "Complementary sliding mode variable structure control for permanent magnet linear synchronous motor," *Proc. CSEE*, vol. 35, no. 10, pp. 2552–2557, May 2015.

[24] F.-J. Lin, J.-C. Hwang, P.-H. Chou, and Y.-C. Hung, "FPGA-based intelligent-complementary sliding-mode control for PMLSM servo-drive system," *IEEE Trans. Power Electron.*, vol. 25, no. 10, pp. 2573–2587, Oct. 2010.

[25] F.-J. Lin, S.-Y. Chen, K.-K. Shyu, and Y.-H. Liu, "Intelligent complementary sliding-mode control for LUSMS-based X-Y-θ motion control stage," *IEEE Trans. Ultrason., Ferroelectr., Freq. Control*, vol. 57, no. 7, pp. 1626–1640, Jul. 2010.

[26] C.-S. Chen and W.-C. Lin, "Self-adaptive interval type-2 neural fuzzy network control for PMLSM drives," *Expert Syst. Appl.*, vol. 39, no. 12, pp. 14679–14689, Nov./Dec. 2011.

[27] S.-Y. Chen, H.-H. Chiang, T.-S. Liu, and C.-H. Chang, "Precision motion control of permanent magnet linear synchronous motors using adaptive fuzzy fractional-order sliding-mode control," *IEEE/ASME Trans. Mechatronics*, vol. 24, no. 2, pp. 741–752, Apr. 2019.

[28] S. A. Nasar and I. Boldea, *Linear Electric Motors: Theory, Design and Practical Applications*. Englewood Cliffs, NJ, USA: Prentice-Hall, 1987.

[29] J.-J. Slotine and W. Li, *Applied Nonlinear Control*. Upper Saddle River, NJ, USA: Prentice-Hall, 1991, pp. 276–306.

[30] S. Mobayen, "Design of CNF-based nonlinear integral sliding surface for matched uncertain linear systems with multiple state-delays," *Nonlinear Dyn.*, vol. 77, no. 3, pp. 1047–1054, Aug. 2014.

[31] K. R. Buckholtz, "Sliding mode control using a switching function incorporating the state trajectory approach angle," Ph.D. dissertation, School Eng., Univ. Dayton, Dayton, OH, USA, 2001.

[32] L. Liu, *Analysis and Design of Sliding Mode Control Systems*. Beijing, China: Science Press, 2017.

[33] F. F. M. El-Sousy and K. A. Abuhasel, "Intelligent adaptive dynamic surface control system with recurrent wavelet Elman neural networks for DSP-based induction motor servo drives," in *Proc. IEEE IAS 52th Annu. Meeting*, Cincinnati, OH, USA, Oct. 2017, pp. 1–16.

HONGYAN JIN was born in Shenyang, Liaoning, China, in 1993. She received the B.S. degree in electrical engineering from the Shenyang University of Technology, Shenyang, in 2016, where she is currently pursuing the Ph.D. degree in electrical engineering. Her research interests include motor control and intelligent control.

XIMEI ZHAO was born in Changchun, Jilin, China, in 1979. She received the B.S., M.S., and Ph.D. degrees in electrical engineering from the Shenyang University of Technology, Shenyang, China, in 2003, 2006, and 2009, respectively, where she is currently a Professor and the Ph.D. Supervisor with the School of Electrical Engineering. She has authored or coauthored more than 100 technical articles and three textbooks. Her research interests include electrical machines, motor drives, motor control, intelligent control, and robot control. She holds 15 patents in these areas.